END FLUX PEAKING STUDY FOR ACR-700-TYPE REACTOR

A. Zkiek
Institut de génie nucléaire, École Polytechnique de Montréal
C.P 6079, succ. Centre-Ville, Montréal, Québec, CANADA, H3C 3A7
email : abdelhamid.zkiek@polymtl.ca

Abstract

The main objective here is to determine the axial profile of the flux along a fuel channel as a function of the fuel bundle burnup taking into account the effect of water interfaces at the end of fuel bundles (end flux peaking). In order to perform these calculations, we have to establish a 3D representation of an ACR reactor channel (each channel contains a set of two to 12 bundles). All these calculations are performed using the transport cell code DRAGON.

The DRAGON calculation procedure we selected is the following: we first perform a 2D calculation to generate homogenized cross sections for annular 2D fuel cells by using a direct or SPH homogenization procedure. No energy condensation is performed. In the second step, we proceed to the 3D calculations for the fuel channel. For our 3D fuel model, we first study the tracking effect to minimize the errors on volumes and surfaces, and then we carry out the calculation of neutron flux. The flux along the z-axis is condensed to 2-energy groups. The effect of fuel burnup on end flux peaking is finally studied.

Introduction

Usually the cell code DRAGON[1] is used to perform the cell calculations using a 2D cell representation of a CANDU lattice. This model implies that the flux is constant along the Z-axis. However this flux has values higher in the extreme parts of the fuel bundle 'End region' than in the inner parts of the fuel bundle 'Fuel region', this effect being called 'End flux peaking'.[2,3] This effect arises because the end regions effectively contain a large amount of coolant compared to the central part of a fuel bundle. The interest of making this kind of calculation is to have information in variation of temperature which depends of the neutron power. End-region flux peaking leads to a higher fission rate, and hence, elevated power and pellet temperatures in the ends of the fuel stack of all fuel elements. This could damage the materials protecting fuel and also part of the fuel itself. Note that this was study was limited to calculating the end-flux peaking; no provision was made to reduce the end-flux peaking.

We have decided to perform this study on end flux peaking on an Advanced CANDU Reactor ACR-700™[*]. To perform this study by using the cell code DRAGON, we selected some 3D models of the fuel bundles. Here we limit our studies to models which treat two neighbour bundles in the axial direction having the same burnup and also two different burnups. A very important parameter called the end flux peaking factor P_0 was calculated to qualify these calculations

1 Modeling

[*] ACR and Advanced CANDU Reactor are trademarks of Atomic Energy of Canada Limited

1.1 2D cell of the ACR-700 reactor

In order to calculate the macroscopic cross sections that will be used for the 3D model of the ACR-700 bundle,[3] we need a multigroup flux distribution (for 89 energy group) inside the 2D calculations of the ACR-700 cell (see figure 1)

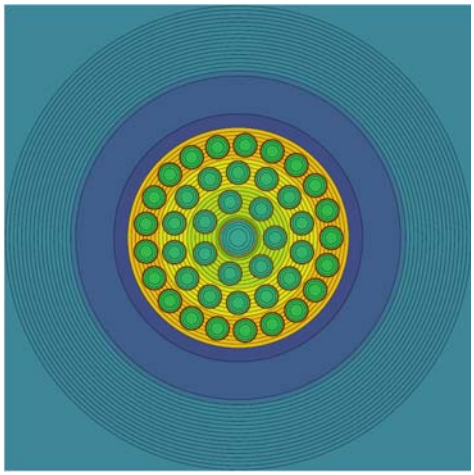

Figure 1: 2D Representation of the ACR-700 cell.

In this model we define the cell geometry and the composition of various mixtures of fuel bundle, coolant, pressure tube, gas gap, calandria and moderator. Before proceeding with the calculations, we correct the cross sections by using the approach of self shielding. Then the neutron flux is computed over the geometry. Finally we homogenize the cross sections by using the SPH method,[4] and by using the EDI module we merge the mixtures that will be used in our 3D models into 8 new mixtures: 4 fuel, pressure tube, gas gap, calandria and one moderator mixtures (see figure 2).

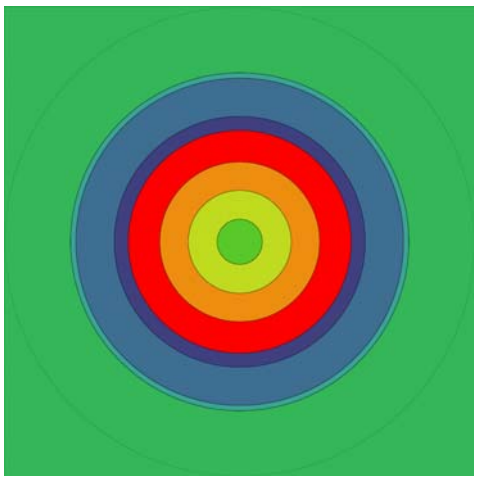

Figure 2: 2D representation of the homogenized ACR cell

1.2 SPH Homogenization

The homogenized cross sections by the method of the direct homogenization are given as:

$$\Sigma_J^h = \frac{\Sigma_{j\in J} V_j \phi_j^h \Sigma_j^h}{\Sigma_{j\in J} V_j \phi_j^h} \quad (1)$$

where Σ_J^h is the homogenized cross section in the supercell region J and Σ_j^h, ϕ_j^h and V_j are respectively the cross section, the flux, and the volume associated with the cell region j in the fine group h.

This method presents some problems: the geometry used in the supercell calculations is different from the one used in the cell calculations, moreover, cell and supercell calculations can be performed using different computational methods (Collision Probability or Method of Characteristics). To avoid this kind of problems, several homogenization techniques are developed, and the one widely used in DRAGON is the SPH homogenization method. In this case the homogenized cross sections will be corrected as:

$$\tilde{\Sigma}_J^H = \mu_j^H \Sigma_J^H \quad (2)$$

where μ_j^H is the SPH factor and $\tilde{\Sigma}_J^H$ is the SPH corrected homogeneous cross section in region J and macrogroup H. The SPH factors are calculated by considering that we have the same reaction rates obtained from both the 2D heterogeneous cluster geometry and 2D homogenized 8-annulus geometry.

1.3 3D models:

In 3D representation, we selected two models for two fuel bundles. In the first model we consider two fuel bundles with the same composition (same burnup), which allows us to reduce the two fuel bundles representation to a model of one fuel bundle with boundary conditions of symmetry on z = 0 (real boundary like a mirror) and reflection (white boundary) on the side of z-positive (see figure 3).

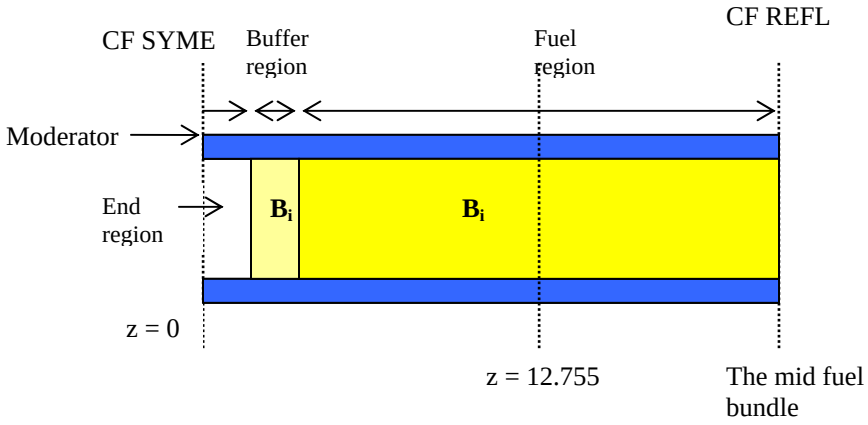

Figure 3: Two fuel bundles model with the same burnup.

The second model contains two fuel bundles with two different burnups with boundary conditions of reflection on both sides of z-negative and z-positive. This representation is similar with the first one but here, we could not reduce it because the two bundles have two different compositions (see figure 4):

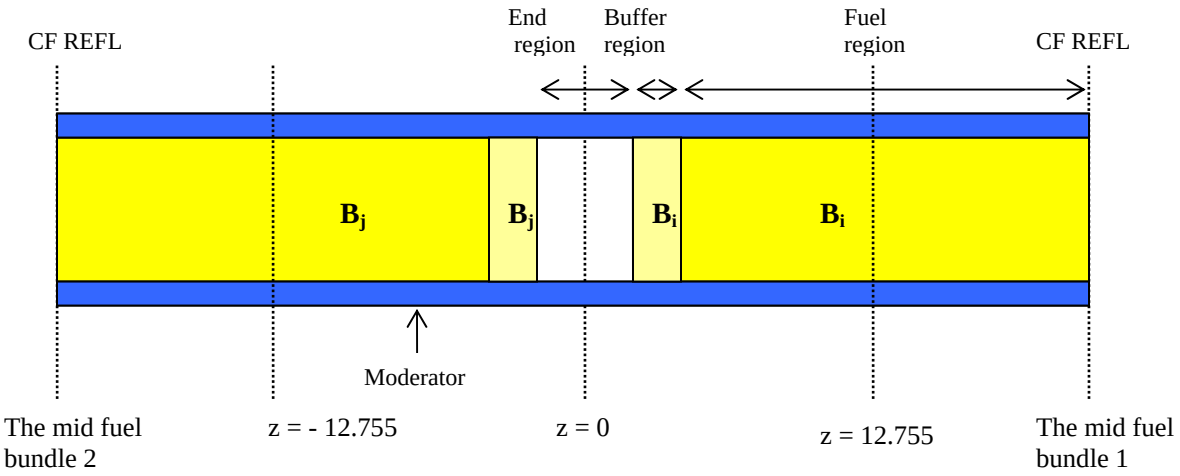

Figure 4: Two fuel bundles model with different burnups.

In these models we divided the fuel bundle into 3 regions:

- The End region is composed of the end cap, the end plate, and the coolant,
- The Buffer region has the same composition as the Fuel region. We separated regions to better see the flux behaviour in the part closer to the end region. The last two regions are composed of the 8 mixtures that we generated using our 2D model.

To obtain the fluxes in these 3D models, we proceed as follows: we use the macroscopic cross sections that we generated in the 2D model, we define the 2 fuel bundles geometry (see figures 3 & 4) and composition, we use the EXCELT module to analyze the chosen geometry (see section 1.5), and finally, the multigroup flux map is obtained by using collision probability techniques. Here we have to point out that we condensed flux calculations into 2 energy groups (cut at 0.625 eV) by using the EDI module. Moreover fluxes in the fuel bundle are homogenized to form a single fuel region.

1.4 DRAGON method calculation :

Before proceeding to 3D calculations, we start with two convergence studies in order to have more reliable and precise results. To minimize the errors on volumes and surfaces, we studied the tracking effect by changing the values of the angular quadrature parameter and the density of the integration lines of the EXCELT module. The results of tracking effect are shown in table 1:

Table 1. K-effective as a function of discretization

Number of angles / Density	K-EFFECTIVE	Δk (mk)
16-160 (reference case)	1.226595	
2-20	1.225741	-0.854
2-40	1.225541	-1.054
4-10	1.226183	-0.412
4-20	1.226531	-0.064
4-30	1.226468	-0.127
4-40	1.226328	-0.267
4-50	1.226291	-0.304
8-20	1.226748	0.153
8-40	1.226549	-0.046
8-80	1.226571	-0.024
8-160	1.226551	-0.044
16-40	1.226586	-0.009
16-80	1.226612	0.017

All further simulations will use the tracking 8-20 because Δk between this tracking and the reference is less than 0.5 *mk*, which also takes less integration lines number as possible. The second study of convergence is carried out to determine the z-discretization in order to minimize errors of calculations to make sure the flux remains stable.

2 Results

2.1 - Model 1: two fuel bundles with the same burnup

2.1.1 Flux profile

To analyze the flux profile, we plot the fast and thermal fluxes for the burnup at 0 GWd/t (see figure 5):

Figure 5 : Flux profile with Burnup = 0

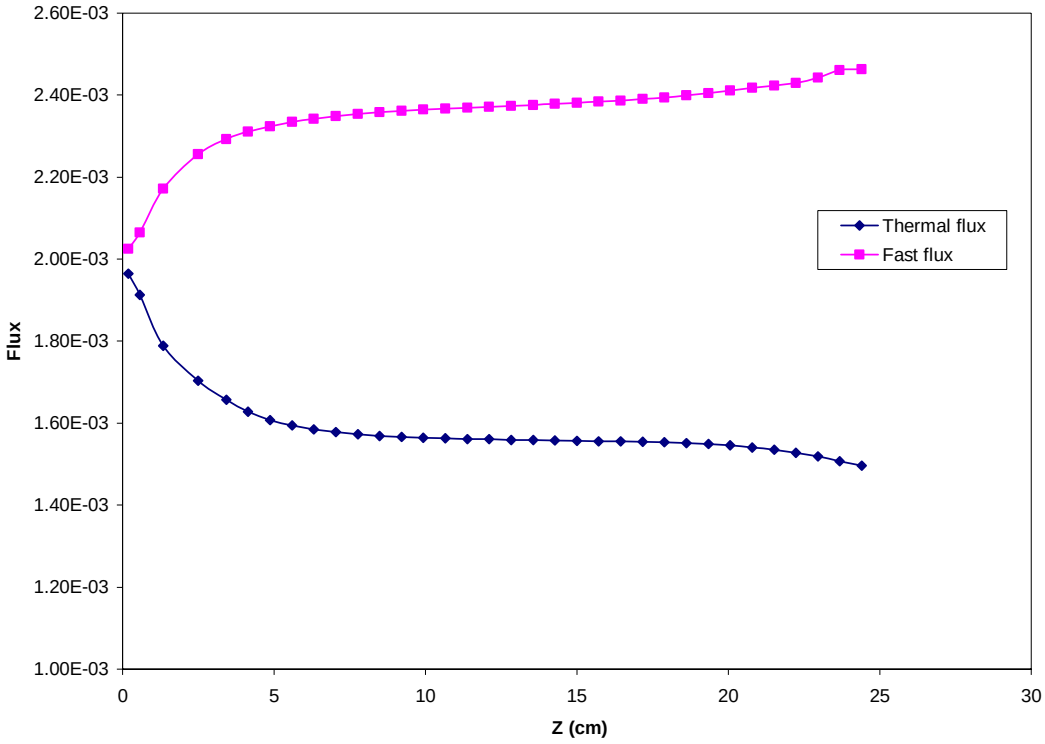

In the two first regions (End and Buffer regions), the fast flux increases; but after that, it remains almost constant in the internal region of the fuel bundle. At mid bundle we see that there is a deviation towards the top due to boundary conditions. We also note that the thermal flux changes inversely to fast flux. In the end region, there is no fuel, which means there is less thermal neutron absorption. In the Buffer region which is close to the end region, the fast neutrons will escape to the end region and will be thermalized by the coolant.

2.1.2 Variation of the thermal flux versus the burnup

The flux is normalized in an arbitrary way: in order to compare thermal fluxes we normalize the thermal fluxes of each burnup by the quarter bundle flux $\phi(12.755\,cm)$ (see figures 3 & 4). Figure 6 shows the variation of end peaking flux (thermal) according to the burnup. We have chosen burnup values up to the maximum burnup required to model an ACR core with a time-average approach.

Figure 6 :Thermal flux vs burnup

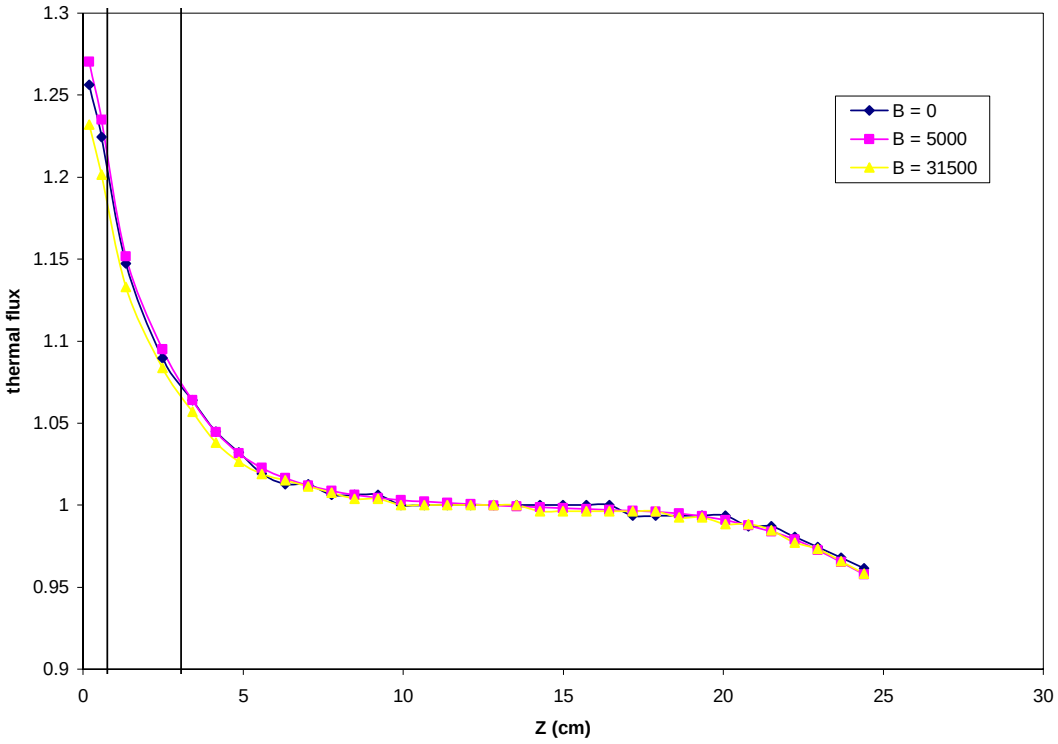

We note that the major difference is observed in the end region. In order to better qualify this difference, we calculate the end flux peaking factors for each burnup. The end flux peaking factor P_0 is defined as:

$$P_o = \frac{\phi_2(0.755cm)}{\phi_2(12.755cm)}$$

where $\phi(0.755\ cm)$ is the end region flux and $\phi(12.755\ cm)$ is the quarter bundle flux. Figure 7 shows the variation of end flux peaking factor according to the burnup.

Figure7: End flux peaking factor versus the burnup

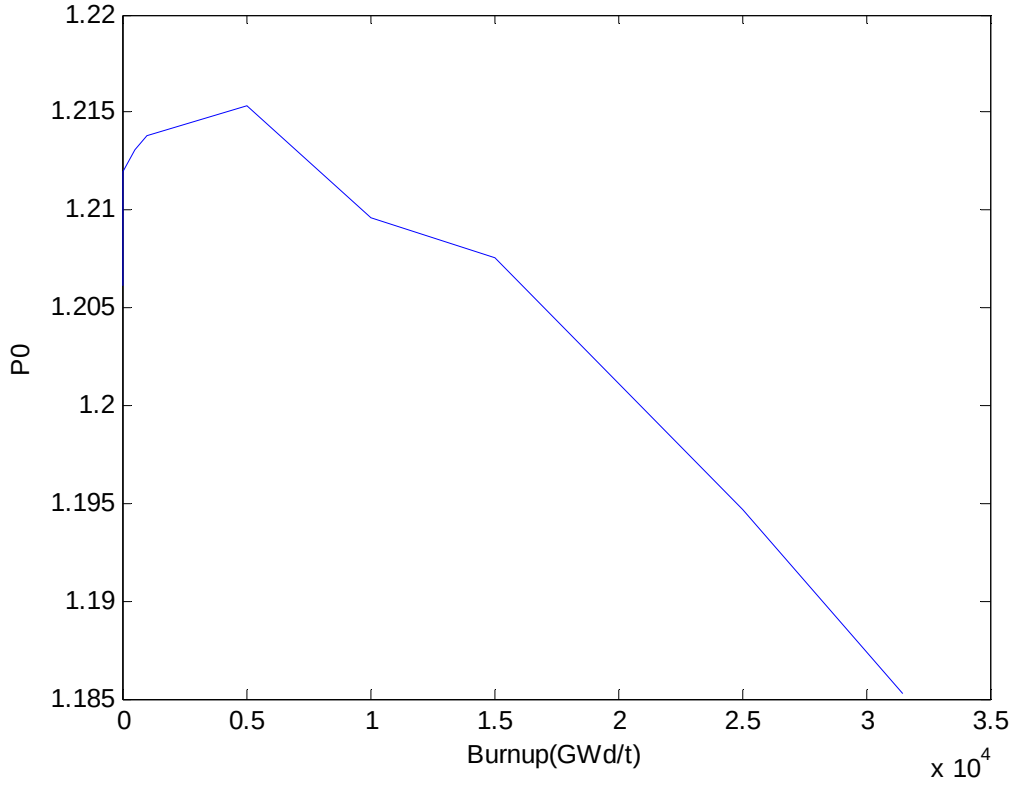

We note a maximum around burnup 5 GWd/t, but after this value of burnup, P_0 decreases. This can be explained by the variation of the quarter bundle flux $\phi(12.755)$ since there is no fuel in the End region. For the bundles which have low burnup, the presence of Dysprosium poison in the centre fuel will decrease the flux. Moreover, for a new bundle ($B = 0$), there is no Xenon poisoning, therefore the quarter bundle flux is higher than that for the bundles with higher burnups. On the other hand, for the high level of burnup, the Dysprosium poison has less effect because of its neutralization. The accumulation of fission products tends to absorb more neutrons thus decreasing the flux in the end region, which means that P_0 will decrease.

2.2 Model 2: two bundles with two different burnups

In this section, we study the variation of the end flux peaking factor P_0 according to the burnup of the 2 neighbouring bundles. Figure 8 gives the variation of the thermal flux for the burnup $B_i = 0$ *GWd/t* and the burnup $B_j = 10$ *GWd/t.* (See Figure 4 for notation)

Figure 8 : B = 0 vs B = 10 GWd/t

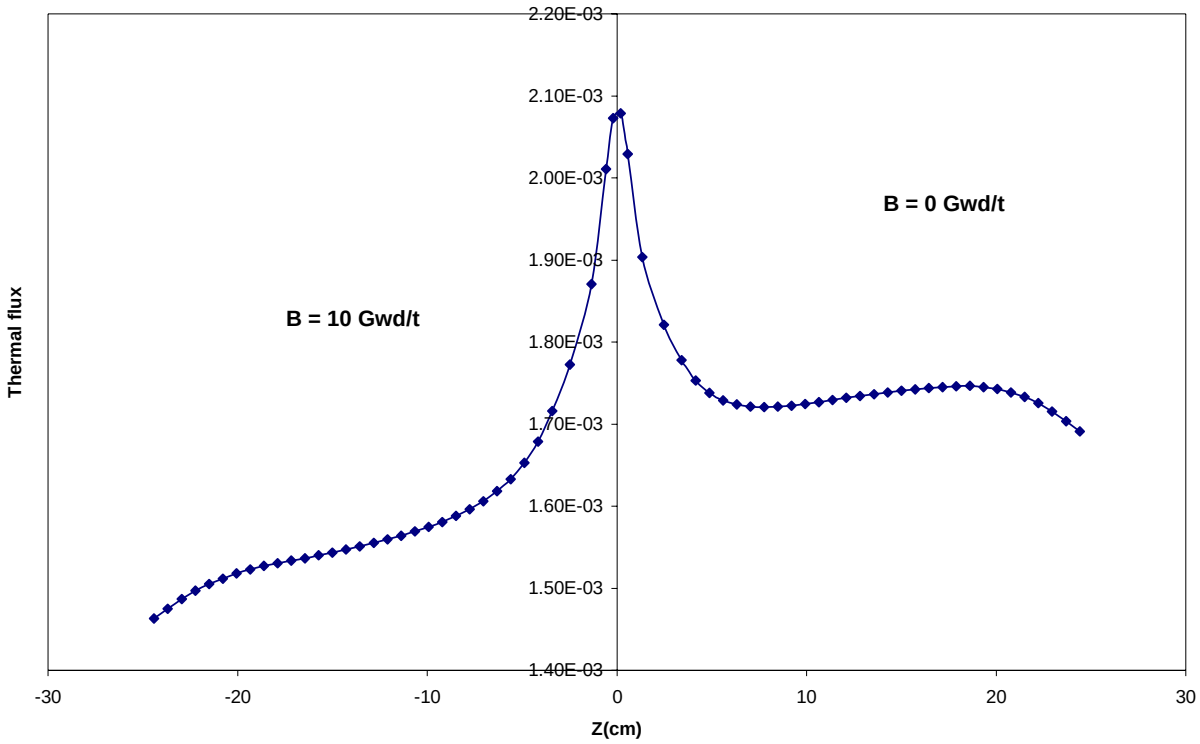

In table 2, we give the variation of P_0 of the burnup B_i and change the burnup B_j:

Table 2. End flux peaking factor for differential burnup bundles

B_i *(GWd/t)*	B_j *(GWd/t)*					
	0	5	10	15	25	31.5
0	1.2061	1.1696	1.1556	1.1432	1.1151	1.1048
10	1.2672	1.2256	1.2096	1.1981	1.1683	-
31.5	1.3043	-	-	-	1.2007	1.1853

We note that for the burnup B_i, the end flux peaking factor P_0 changes according to the burnup B_j of the neighbour bundle. When the burnup B_j increases, the end flux peaking factor decreases.

There is a difference between the P_0 values of (0-10) and (10-0) 2-burnups. In the first case (0-10) burnups, we calculate the end flux peaking factor P_0 on the right hand side of the curve (z-positive) (see figure 8), however, in the second case (10-0) burnups we calculate P_0 on the left hand of the curve (z-negative).

When the B_i increases, the end flux peaking factor increases too, because these values of P_0 are calculated on the left hand side (z-negative) which behaves inversely that the ones we calculated on the right hand side (z-positive).

Conclusion

We studied the end peaking flux and we calculated the end flux peaking factors by using the 3D representation of the fuel bundles of the ACR reactor, this study is seldom treated in the literature. The study of variation of end flux peaking factor according to burnup gives an idea on the flux variation in time. This flux is linked to power and temperature, therefore a high peaking factor P_0 means the temperature in the end region is high, which could damage materials and fuel in this region.

This study was limited to perform models for only two fuel bundles; for future work, it would be interesting to perform models for the whole channel (12 fuel bundles), and also study the refuelling effect on the end flux peaking.

Acknowledgments

This work was supported in part by a grant from the Natural Sciences and Engineering Research Council of Canada, Atomic Energy of Canada Ltd, and by the Hydro-Québec Chair in Nuclear Engineering. Special thanks to Wei Shen from AECL for his valuable comments.

REFERENCES

1. G. Marleau, A. Hébert, and R. Roy, "A User's Guide for DRAGON", Report IGE-174 Rev. 5, Ecole Polytechnique de Montréal, 2005.
2. P.M. French, "Measurement of Bundle End Flux Peaking Effects in 37-element CANDU PHW Fuel," Report AECL-5968, Chalk River Nuclear Laboratories, 1977.
3. W. Shen, "Validation of DRAGON End-Flux Peaking and Analysis of End-Power-Peaking Factors for 37-Element, CANFLEX and Next-Generation CANDU Fuels", 22nd Annual CNS Conference, Toronto, 2001.
4. D.F. Torgerson, "The ACR-700 – Raising the Bar for Reactor Safety, Performance, Economics and Constructability," Nucl. News, 24-32, October 2002.
5. A. Hébert, "A Consistent Technique for Pin-by-Pin Homogenization of a Pressurized Water Reactor Assembly", Nucl. Sci. Eng. **113**, 227, 1991